Prediction of the spectrum for excitation of the van der Waals modes in ArHCN

D. C. Clary, C. E. Dateo, and T. Stoecklin

Citation: The Journal of Chemical Physics **93**, 7666 (1990); doi: 10.1063/1.459398
View online: http://dx.doi.org/10.1063/1.459398
View Table of Contents: http://scitation.aip.org/content/aip/journal/jcp/93/11?ver=pdfcov
Published by the AIP Publishing

Prediction of the spectrum for excitation of the van der Waals modes in ArHCN

D. C. Clary, C. E. Dateo, and T. Stoecklin
Department of Chemistry, University of Cambridge, Lensfield Road, Cambridge CB2 1EW, United Kingdom

(Received 14 June 1990; accepted 7 August 1990)

A calculation of the spectrum for the excitation of the van der Waals modes in ArHCN is reported. The coupled electron pair approximation is used to compute an *ab initio* potential energy surface for the interaction of Ar with rigid HCN. The rovibrational bound states for the complex are calculated using a variational coupled-basis set method in which a self-consistent field approach is used to optimize simultaneously the basis sets for both the intermolecular bending and stretching motions in the van der Waals molecule. The calculations are compared with experimental results, including a measurement of the infrared spectrum of ArHCN in the region of the CH stretching vibration. The calculations predict that several bending modes with frequencies less than 20 cm^{-1} should have excitation intensities large enough to be observed. These low frequency bending modes arise from the small rotational constant of the HCN molecule and are not due to special features of the Ar–HCN potential energy surface.

I. INTRODUCTION

There has been remarkable progress recently in the measurement of spectra for van der Waals complexes at low temperatures.[1] In particular, far and near-infrared spectra on complexes containing infrared active monomers have yielded a wealth of data on the position, intensities, and widths of the spectral lines of these systems.[2] In turn, data of this kind are being used to construct highly accurate potential energy surfaces for a range of molecules.[3–7]

The rare gas–hydrogen halide complexes have been the subject of particularly intensive study,[8–16] and this work is culminating in an almost complete, quantitative understanding of the spectra and potential energy surfaces for many of these particular systems.[3–7] The rare gas–hydrogen halide systems studied to date are all weakly bound by less than 200 cm^{-1} and many have potential energy surfaces with local minima for the rare gas atoms situated at both ends of the hydrogen halide molecule. The large rotational constants of the hydrogen halide monomers ensure well resolved, largely uncongested van der Waals spectra and also enable good quality calculations of the low-frequency rovibrational states of these systems to be calculated from given potential energy surfaces.

It might be expected that the complexes of rare gases with HCN have quite similar spectra to those for the rare gas–HCl complexes. The microwave spectra for ArHCN and KrHCN are characteristic of linear molecules,[17,18] although the centrifugal distortion constants are found to be surprisingly large and the spectra are found to be unusually sensitive to substitution of the H atom by a deuterium atom.[18] Furthermore, the measured ^{14}N quadrupole constants for ArHCN suggest very large zero-point bending amplitudes.[18] Klots *et al.* examined the J dependence of the quadrupole coupling constant for ArHCN in detail.[19] They found that the dependence of the amplitude of the ArHCN fundamental mode on bending angle decreased much more significantly with total angular momentum J than that observed for ArHCl and ArHBr.

Klots *et al.* also calculated an electrostatic potential for the region close to the collinear Ar–HCN configuration.[19] They found a minimum in the potential at an angle of 16° displaced from the collinear geometry with a very weak dependence of the potential on angle in this region. This leads to the ground state wave function sampling the linear configuration for large values of the Ar–HCN intermolecular distance R, and the noncollinear configuration for smaller R, also implying strong angular–radial coupling. However, this potential was not calculated over a large number of configurations that would enable a global potential energy surface to be fitted that is appropriate for calculations of the rovibrational energy levels and spectra for the van der Waals modes in ArHCN. Even more comprehensive microwave experiments on ArHCN have been reported recently by Bumgarner and Blake who measured transitions up to $J = 19 \rightarrow 20$, and confirmed the very strong centrifugal distortion of the fundamental energy level in this system.[20]

Some of the experimental data on ArHCN has been explained by Leopold *et al.* in terms of a model potential energy surface that has local minima for both the linear and T-shaped ArHCN configurations separated by a small barrier.[18] This potential produces the strong angular–radial coupling that is suggested by the experimental findings. Leopold *et al.* also used their model to estimate that the bending and stretching frequencies of the van der Waals modes in ArHCN are about 10 cm^{-1}.

In contrast with the rare gas–hydrogen halide systems, there have been no absolutely certain assignments of low frequency bending vibrations in rare gas–HCN complexes. However, in measurements of the infrared spectrum involving excitation of the C–H stretching vibration in ArHCN, Fraser and Pine did recently observe a combination band displaced about 8 cm^{-1} from the C–H stretch frequency that they suggested might be associated with an excited van

 0021-9606/90/237666-10$03.00

der Waals bending mode.[21]

In a series of recent calculations on weakly bound complexes including NeHF,[15] H_2HF,[22] and ArOH,[23] we and co-workers have done extensive correlated *ab initio* calculations of points on the potential energy surfaces, followed by a fit of a potential energy function to these points and variational calculations of the rovibrational bound states and spectra for the van der Waals modes.[24] These calculations have shown that such first-principles calculations play a useful role in predicting the general features of the spectrum, including the relative magnitudes of the frequencies, intensities, and, in special cases, widths of the spectral lines for the low frequency van der Waals modes. Indeed, some of our predictions of unusual features in the spectra of van der Waals molecules have already been confirmed in experiments.[15] These calculations cannot be expected to give results that compare with the accuracy of high resolution spectroscopy but they play a valuable role in understanding the basic features of the spectra of van der Waals molecules in cases where the experiments are uncertain or have not been performed.

Given the intensive current interest in ArHCN and the fact that this system is far from being well understood, it is clearly valuable to attempt an *ab initio* calculation of the spectrum for excitation of the van der Waals modes in this system. Here we report such a computation. The *ab initio* calculations are done using the coupled electron-pair approximation (CEPA-1)[25] with a large basis set. 112 points on the potential energy surface are calculated, with the HCN monomer held fixed as a rigid rotor, and this is sufficient to produce a potential energy function for the Ar + HCN interaction. The rovibrational bound states are then calculated by using a variational basis set method that involves performing self-consistent field calculations[26,27] to produce optimum basis sets for the intermolecular bending and stretching motions in the ArHCN complex, and then using these basis sets in a final configuration-interaction calculation of the rovibrational states. By assuming that the dipole moment of ArHCN is directed along the HCN bond we are then able to predict the spectrum for excitation of the van der Waals modes. Furthermore, with the assumption that the van der Waals levels hardly change when the CH vibrational mode is excited, the predictions should also be relevant for the infrared spectra that involve excitation of the CH stretching vibration in ArHCN.

The approximation of treating the molecular monomer as a rigid linear rotor in the *ab initio* and rovibrational bound state calculations has been shown to work well in calculations on related systems to ArHCN such as NeHF[15] and ArOH,[23] while the approximation of placing the dipole moment of the van der Waals complex along the direction of the dipole of the infrared-active monomer gives good results for several complexes, including NeHF,[15] NeHCl,[14] ArHCl,[14] H_2HF,[22] and $(HF)_2$.[28]

In Sec. II we briefly describe the *ab initio* computations and fit of the potential energy function. We also discuss the method for calculating the rovibrational bound states of ArHCN. Numerical aspects of these computations are presented in Sec. III. Section IV reports our predictions of the energy levels and spectra, and the results are compared with the available experimental data. Conclusions are in Sec. V.

II. CALCULATIONS

A. *Ab initio* computations and potential energy surface

The *ab initio* calculations were done with the CEPA-1 method with a large basis set of contracted Gaussians: H(10*s* 2*p*/7*s* 2*p*), C(11*s* 7*p* 3*d*/6*s* 4*p* 3*d*), N(11*s* 7*p* 3*d*/6*s* 4*p* 3*d*), Ar(14*s* 10*p* 3*d*/10*s* 7*p* 3*d*). Some diffuse orbitals were included in the basis set as suggested by the calculations of Ref. 15. The exponents of these basis functions were optimized to give a value of 2.966 D for the calculated dipole moment of HCN that agrees well with the experimental value of 2.984 D.[29] The calculated HCN isotropic polarizability with this basis set was 2.458 Å^3, which compares well with the experimental value[29] of 2.59 Å^3. The C and N 1*s* orbitals and Ar 1*s*, 2*s*, and 2*p* orbitals were treated as core in the CEPA-1 wave function. The bond lengths in linear HCN were set at 1.064 Å for CH and 1.156 Å for CN in these computations. Since the HCN bending and stretching vibrational frequencies are over two orders of magnitude larger than the frequencies of the bending and stretching van der Waals modes in ArHCN, it seems appropriate to fix the HCN molecule as a rigid rotor in both the *ab initio* and rovibrational bound state calculations. The experimental infrared spectra on ArHCN suggest that vibrational predissociation is very inefficient in this system implying only weak coupling between the van der Waals modes and the CH stretching mode.[21] The coupling with the vibrational bending mode of HCN is likely be stronger than that for the CH stretch but the differences in frequency should ensure that neglect of the HCN bending mode in all the calculations is still a good approximation. Thus we expect that the van der Waals modes for the Ar–HCN ground state should be very similar to those for Ar–HCN with one vibrational quantum in the CH stretching vibration.

Since we are not allowing the HCN molecule to bend, coordinates appropriate for an atom–linear molecule interaction are appropriate[30] for the Ar + HCN interaction. Thus, **R** is the vector that joins the Ar atom to the center of mass of the HCN molecule, **r** is the vector along the HCN bond, and θ is the angle of orientation of **R** with respect to **r**, with $\theta = 0°$ corresponding to the Ar atom being closer to the H atom than the N atom. The *ab initio* calculations were done at 112 geometries of Ar + HCN, with θ taking 30° intervals between 0° and 180° and R having intervals between 6.5 and 11.0 bohr. Basis set superposition errors were accounted for by employing the usual counterpoise correction.[31] The potential for the Ar + HCN interaction was expanded in the form

$$V(R,\theta) = \sum_{n=0}^{6} c_n(R) P_n \cos(\theta), \tag{1}$$

where $P_n \cos(\theta)$ is a Legendre polynomial and

$$c_n(R) = \left[\sum_{k=0}^{3} x_k^n R^k \exp(-2R)\right] + \frac{x_4^n}{R^6}\left\{1 - \exp\left[-\left(\frac{R}{3}\right)^8\right]\right\}, \tag{2}$$

TABLE I. Coefficients in the potential energy surface expansion for Ar + HCN in atomic units [see Eq. (2)].

n	x_0^n	x_1^n	x_2^n	x_3^n	x_4^n
0	− 23.3	− 789	325	− 25.4	− 113
1	− 342	− 606	266	− 21.1	− 19.8
2	28.6	− 811	425	− 35.6	− 63.1
3	− 20.3	− 774	320	− 25.6	− 15.7
4	− 171	− 468	251	− 21.3	− 7.27
5	− 118	− 344	175	− 14.9	− 2.91
6	− 2.49	− 648	223	− 17.2	0.469

where R is in units of bohr. The radial part of the potential energy function used is of a standard form with a polynomial multiplied by an exponential function for the short-range term and a damped attractive $1/R^6$ term for the long-range part.[22] It was found in trial least-squares fits to the *ab initio* points that the exponent in the short range part of the potential function expansion was always very close to $-2\,\text{bohr}^{-1}$ and hence it was fixed at this value. The 35 coefficients $\{x_k^n\}$ defined in Eq. (2), which were obtained as a least-squares fit to the 112 *ab initio* points, are given in Table I. Table II gives the *ab initio* points and the values of the potential function at those points. It can be seen that, around the minimum in the potential, the agreement is good for each point to within 2 cm^{-1}, and is mostly much better than that.

The potential energy surface has a minimum interaction

TABLE II. *Ab initio* and fitted energy points for the Ar + HCN interaction in units of cm^{-1}.

R/a_0	$\theta°$	*Ab initio*	Fit	[*Ab initio* − Fit]
6.50	0	4352.181	4368.595	− 16.414
	30	1694.890	1738.996	− 44.106
	60	212.794	190.634	22.160
	90	58.757	32.100	26.657
	120	151.715	160.327	− 8.612
	150	616.241	627.095	− 10.854
	180	1049.940	1085.527	− 35.587
6.75	0	2552.260	2575.105	− 22.845
	30	966.560	986.379	− 19.819
	60	78.741	70.983	7.758
	90	− 6.845	− 19.104	12.259
	120	41.480	51.000	− 9.520
	150	314.009	314.171	− 0.162
	180	573.831	590.122	− 16.291
7.00	0	1444.621	1460.618	− 15.997
	30	516.634	524.002	− 7.368
	60	2.217	− 0.258	2.475
	90	− 41.161	− 46.858	5.697
	120	− 19.469	− 12.344	− 7.125
	150	134.094	130.883	3.211
	180	285.887	292.015	− 6.128
7.25	0	774.678	782.537	− 7.859
	30	245.404	247.243	− 1.839
	60	− 38.713	− 39.521	0.808
	90	− 56.771	− 59.531	2.760
	120	− 50.446	− 46.018	− 4.428
	150	30.795	27.412	3.383
	180	116.359	117.767	− 1.408
7.50	0	377.659	380.093	− 2.434
	30	87.034	87.013	0.021
	60	− 58.112	− 58.508	0.396
	90	− 61.555	− 62.991	1.436
	120	− 63.663	− 61.282	− 2.381
	150	− 25.365	− 27.780	2.415
	180	20.226	19.926	0.300
7.75	0	148.523	148.660	− 0.137
	30	− 1.239	− 1.500	0.261
	60	− 64.948	− 65.198	0.250
	90	− 60.371	− 61.174	0.803
	120	− 66.730	− 65.630	− 1.100
	150	− 53.127	− 54.404	1.277
	180	− 31.148	− 31.716	0.568
8.00	0	21.396	21.287	0.109
	30	− 46.961	− 46.868	− 0.093
	60	− 64.642	− 64.834	0.192
	90	− 56.153	− 56.614	0.461
	120	− 64.288	− 63.887	− 0.401
	150	− 64.253	− 64.615	0.362
	180	− 55.834	− 56.104	0.270
8.25	0	− 44.647	− 44.166	− 0.481
	30	− 67.509	− 66.996	− 0.513
	60	− 60.650	− 60.744	0.094
	90	− 50.626	− 50.876	0.250
	120	− 59.287	− 59.059	− 0.228
	150	− 66.007	− 65.784	− 0.223
	180	− 65.063	− 64.925	− 0.138
8.50	0	− 74.940	− 73.781	− 1.159
	30	− 73.752	− 72.900	− 0.852
	60	− 54.974	− 54.963	− 0.011
	90	− 44.769	− 44.881	0.112
	120	− 53.174	− 52.950	− 0.224
	150	− 62.846	− 62.299	− 0.547
	180	− 65.705	− 65.261	− 0.444
8.75	0	− 84.955	− 83.406	− 1.549
	30	− 72.206	− 71.224	− 0.982
	60	− 48.779	− 48.681	− 0.098
	90	− 39.113	− 39.134	0.021
	120	− 46.990	− 46.589	− 0.401
	150	− 57.343	− 56.708	− 0.635
	180	− 61.909	− 61.311	− 0.598
9.00	0	− 84.203	− 82.477	− 1.726
	30	− 66.846	− 65.872	− 0.974
	60	− 42.704	− 42.555	− 0.149
	90	− 33.919	− 33.885	− 0.034
	120	− 41.200	− 40.527	− 0.673
	150	− 51.001	− 50.440	− 0.561
	180	− 56.109	− 55.495	− 0.614
9.50	0	− 69.841	− 68.446	− 1.395
	30	− 52.659	− 52.030	− 0.629
	60	− 32.019	− 31.883	− 0.136
	90	− 25.233	− 25.171	− 0.062
	120	− 31.481	− 30.167	− 1.314
	150	− 38.748	− 38.530	− 0.218
	180	− 43.366	− 42.999	− 0.367
10.00	0	− 52.827	− 52.139	− 0.688
	30	− 39.458	− 39.341	− 0.117
	60	− 23.727	− 23.710	− 0.017
	90	− 18.737	− 18.690	− 0.047
	120	− 22.666	− 22.349	− 0.317
	150	− 28.782	− 28.928	0.146
	180	− 32.335	− 32.344	0.009
11.00	0	− 28.293	− 28.930	0.637
	30	− 21.505	− 22.180	0.675
	60	− 13.234	− 13.364	0.130
	90	− 10.528	− 10.567	0.039
	120	− 12.088	− 12.554	0.466
	150	− 15.993	− 16.437	0.444
	180	− 17.710	− 18.271	0.561

energy of $-84.955\ cm^{-1}$ at $R = 8.75$ bohr and $\theta = 0°$. It can also be seen from the points in the table that, in this region of R, the potential has local minima at 0° and 180° with a local maximum at 90°. This is reminiscent of the potentials for rare gas–hydrogen halide complexes such as ArHCl and ArHF.[4,7] Figure 1 gives plots of the potential as a function of θ for different values of R. We also did some extra *ab initio* calculations for values of θ up to 30°, but found that the minimum in the potential was still at 0° and did not see the features found by Klots *et al.* who calculated a minimum at 16.1°.[19]

Basis set superposition errors are significant in this system. For example if they are not included, the minimum in the potential is at the same geometry as when they are included ($R = 8.75$ bohr, $\theta = 0°$) but the interaction energy decreases from -84.95 to $-124.53\ cm^{-1}$. Comparison of similar *ab initio* calculations on ArHCl with an experimentally determined potential suggests that the actual energy should be between these two values.[32] We also did extra *ab initio* calculations by extending the basis set in which an f orbital was added to the Ar atom. The minimum in the potential then moved to $R = 8.5$ bohr for the collinear configuration with an energy of $-98.632\ cm^{-1}$. As this is only a small difference between the value calculated with the smaller basis it did not seem worthwhile to perform the much more expensive calculations with the larger basis to produce the entire potential energy surface.

B. Rovibrational bound state calculations

The calculations of the rovibrational bound states were done by adapting a method that we have applied before to the H_2HF system.[22] The full rovibrational Hamiltonian is written as

$$H = H_{\text{stretch}} + H_{\text{bend}} + l^2/(2\mu R^2) + H_{\text{couple}}, \tag{3}$$

where

$$H_{\text{stretch}} = -\frac{\hbar^2}{2\mu}\frac{\partial^2}{\partial R^2} + V_{\text{stretch}}(R), \tag{4}$$

$$H_{\text{bend}} = b\mathbf{j}^2 + gl^2 + V_{\text{bend}}(\theta), \tag{5}$$

and

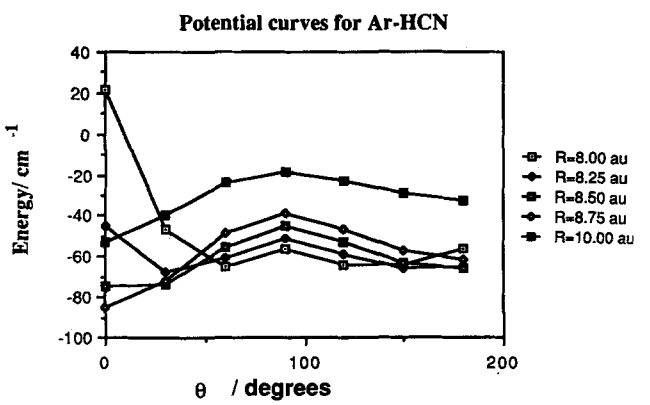

FIG. 1. *Ab initio* calculations of points on the potential energy surface for the Ar + HCN interaction. Plots of energies are presented as a function of θ for different values of R. $\theta = 0°$ corresponds to the collinear Ar–HCN configuration.

$$H_{\text{couple}} = V(R,\theta) - V_{\text{stretch}}(R) - V_{\text{bend}}(\theta) - gl^2. \tag{6}$$

Here, $\mathbf{j}^2$ and l^2 are the angular momentum operators associated with the rotation of **r** and **R**, respectively, in the space-fixed coordinate frame,[30] b is the rotational constant for rigid HCN and μ is the collisional reduced mass. The stretching and bending potentials $V_{\text{stretch}}(R)$ and $V_{\text{bend}}(\theta)$, and g, an average over $1/(2\mu R^2)$, are all defined below.

It is necessary to find the eigenvalues of the full Hamiltonian H of Eq. (3). To do this, appropriate basis sets have to be calculated for the stretching and bending motions independently. An SCF-CI procedure is applied to do this.[22] First of all, $V_{\text{stretch}}(R)$ is set equal to $c_0(R)$ of Eq. (1). Then H_{stretch} is diagonalized with a basis set of n_t distributed Gaussian functions[33]

$$\Psi^k_{\text{stretch}}(R) = \sum_i^{n_t} d_i^k \exp[-\alpha(R - R_i)^2] \tag{7}$$

which are equally spaced on a grid of R_i values ranging between R_a and R_b. This gives a basis set of stretching wave functions $\{\Psi^k_{\text{stretch}}(R), k = 1,...,n_t\}$ with corresponding eigenvalues $\{\epsilon^k_{\text{stretch}}, k = 1,...,n_t\}$. The common exponent α is varied to produce a minimum energy for the stretching wave function with lowest energy (i.e., $k = 1$). This stretching wave function $\Psi^1_{\text{stretch}}(R)$ is then used to average over $V(R,\theta)$ to produce the bending potential $V_{\text{bend}}(\theta)$.

Next, the bending Hamiltonian of Eq. (5) with

$$g = \left\langle \Psi^1_{\text{stretch}}(R) \left| \left(\frac{1}{2\mu R^2}\right) \right| \Psi^1_{\text{stretch}}(R) \right\rangle$$

and

$$V_{\text{bend}}(\theta) = \langle \Psi^1_{\text{stretch}}(R) | \{V(R,\theta) - V_{\text{stretch}}(R)\} | \Psi^1_{\text{stretch}}(R) \rangle \tag{8}$$

is diagonalized by using the angular basis set

$$\mathcal{Y}^{JMp}_{lj}(\theta',\phi',\theta'',\phi'') = \sum_{m_j}\sum_{m_l} C(j,l,J,m_j,m_l,M) \times Y_j^{m_j}(\theta',\phi') Y_l^{m_l}(\theta'',\phi''), \tag{9}$$

where the C's are Clebsch–Gordon coefficients and the Y's are spherical harmonics.[34] The angles (θ',ϕ') and (θ'',ϕ'') describe the orientation of **r** and **R**, respectively, in the space-fixed frame. This diagonalization is done for a fixed value of the total angular momentum J and parity p, where $p = (-1)^{j+l}$. The projection quantum number of the total angular momentum along the space-fixed z axis is M, and this is set to the arbitrary value of 0 in the eigenvalue calculations. In the basis set used for the diagonalization of H_{bend}, j takes the maximum value $j_{\max}$ and, for each j, l takes all values allowed by

$$|J - j| \leqslant l \leqslant |J + j|.$$

This gives the bending basis functions $\{\Psi^{k'Jp}_{\text{bend}}\}$ with eigenvalues $\{\epsilon^{k'Jp}_{\text{bend}}\}$. The secular matrix that needs to be diagonalized to produce these bending wave functions has the elements between the basis functions (j,l) and (j',l'),

$$[bj(j+1)+gl(l+1)]\delta_{jj',ll'}$$
$$+\sum_{n=1}\langle\Psi^1_{\text{stretch}}(R)|c_n(R)|\Psi^1_{\text{stretch}}(R)\rangle$$
$$\times(-1)^{l+l'+J}[(2j+1)(2j'+1)(2l+1)$$
$$\times(2l'+1)]^{1/2}$$
$$\times\begin{pmatrix}l & n & l'\\ 0 & 0 & 0\end{pmatrix}\begin{pmatrix}j & n & j'\\ 0 & 0 & 0\end{pmatrix}\begin{Bmatrix}l & n & l'\\ j' & J & j\end{Bmatrix}. \quad (10)$$

Once these bending eigenfunctions are obtained the next iteration in the SCF procedure is applied by averaging over the potential with the bending basis function of lowest energy to yield an updated form for $V_{\text{stretch}}(R)$,

$$V_{\text{stretch}}(R)=\langle\Psi^{k'=1JpM}_{\text{bend}}|V(R,\theta)|\Psi^{k'=1JpM}_{\text{bend}}\rangle \quad (11)$$

and H_{stretch} is diagonalized again to produce a new stretching basis $\{\Psi^k_{\text{stretch}}(R)\}$. The stretching basis function that has lowest energy is then used to construct the bending potential of Eq. (8) to produce another set of bending wave functions $\{\Psi^{k'JpM}_{\text{bend}}\}$. In turn, the whole SCF procedure can be repeated as many times as required until the bending and stretching eigenvalues of interest hardly change. The final basis functions are then $\{\Psi^{k'JpMf}_{\text{bend}}\}$ and $\{\Psi^{kf}_{\text{stretch}}\}$ and the final value of g is g^f. The final bending and stretching potentials are $V^f_{\text{bend}}(\theta)$ and $V^f_{\text{stretch}}(R)$, respectively.

When the optimum bending and stretching basis functions have been obtained with this SCF procedure, the full Hamiltonian H of Eq. (3) is then diagonalized with the coupled configuration-interaction (CI) expansion

$$\Psi^{nJpM}(R,\theta',\phi',\theta'',\phi'')=\sum_k\sum_{k'}d^{nJpM}_{kk'}\Psi^{k'JpMf}_{\text{bend}}$$
$$\times(\theta',\phi',\theta'',\phi'')\Psi^{kf}_{\text{stretch}}(R). \quad (12)$$

The secular matrix that needs to be diagonalized has the elements between the basis functions (k_a,k'_a) and (k_b,k'_b):

$$\left(\epsilon^{k_af}_{\text{stretch}}+\epsilon^{k'_aJpMf}_{\text{bend}}\right)\delta_{k_ak_b,k'_ak'_b}$$
$$+\left\langle\Psi^{k_af}_{\text{stretch}}\Psi^{k'_aJMpf}_{\text{bend}}\right|\left[\frac{l^2}{2\mu R^2}-g^f+V(R,\theta)\right.$$
$$\left.-V^f_{\text{stretch}}(R)-V^f_{\text{bend}}(\theta)\right]|\Psi^{k_bf}_{\text{stretch}}\Psi^{k'_bJMpf}_{\text{bend}}\rangle. \quad (13)$$

The SCF procedure can be used for each value of J if necessary, although often a calculation of the stretching basis set for $J=0$ will suffice. The basis set is kept to a reasonable size by imposing the restrictions $k\leqslant N_{\text{stretch}}, k'\leqslant N_{\text{bend}}$, and $k+k'\leqslant N_X$ for $k,k'>3$. The integers $N_{\text{stretch}}, N_{\text{bend}}$, and N_X are varied to enable the convergence of the calculated energy levels to be examined.

The intensities for the transition $nJpM\rightarrow n'J'p'M$, with $p\neq p'$, are easily calculated with the approximation that the dipole lies along the HCN monomer.[24] The transition amplitudes are then

$$A(n,J,p,M)\rightarrow n',J',p',M)=|\langle\Psi^{nJpM}(R,\theta',\phi',\theta'',\phi'')|$$
$$\times Y^0_1(\theta',\phi')|\Psi^{n'J'p'M}$$
$$\times(R,\theta',\phi',\theta'',\phi'')\rangle|^2. \quad (14)$$

The basic matrix elements that first need to be computed are

$$\langle\mathscr{Y}^{JMp}_{lj}(\theta',\phi',\theta'',\phi'')\,|\,Y^0_1(\theta',\phi')\,|\,\mathscr{Y}^{J'Mp}_{l'j'}(\theta',\phi',\theta'',\phi'')\rangle$$
$$=\delta_{(l,l')}\sum_{m_j}\delta_{(m_l,M-m_j)}C(j,l,J,m_j,m_l,M)$$
$$\times C(j',l',J',m_j,m_l,M)\left[\frac{3(2j'+1)}{(2j+1)}\right]^{1/2}$$
$$\times C(j',1,j,m_j,0,m_j)C(j',1,j,0,0,0) \quad (15)$$

and transformation with the appropriate final eigenvector coefficients gives the transition amplitudes. It follows directly from Eq. (15) that the selection rules

$$J\rightarrow J\pm1,\quad J\rightarrow J\neq0,\quad p\rightarrow p'\neq p$$

are obeyed. The summation of the transition amplitudes over the M quantum number is carried out, and, for a given temperature T of the Ar–HCN complex, a Boltzmann weighting is then carried out with respect to the energy of the initial state (n,J,p).

The above procedures enables a calculation to be carried out of the spectrum for exciting the van der Waals modes in ArHCN in the low frequency range of 0 to 25 cm^{-1}. The infrared spectrum can also be simulated simply by adding the van der Waals frequencies to the frequency of the Ar–HCN fundamental in which the CH stretch is excited. The very low rotational constant of the ArHCN complex, $\sim$0.05 cm^{-1}, ensures a highly congested spectrum unless measurements are made at a very low temperature. The infrared experiments[21] were performed for an ArHCN internal temperature of 1.6 K and our spectra reported here are also for that temperature. This required calculations with J taking values up to 7 for a realistic simulation.

Useful quantities for comparing with experimental data are the average values of $P_1(\cos\theta)$ and $P_2(\cos\theta)$ for each mode n. These are calculated from

$$\langle P_i(\cos\theta)\rangle=\langle\Psi^{nJpM}(R,\theta',\phi',\theta'',\phi'')|$$
$$\times P_i(\cos\theta)|\Psi^{nJpM}(R,\theta',\phi',\theta'',\phi'')\rangle. \quad (16)$$

These results also give direct information of the localization of the rovibrational wave functions. Thus $\langle P_1(\cos\theta)\rangle=1$ corresponds to rigid collinear Ar–HCN, with the Ar placed at the H atom end of the HCN, while $\langle P_1(\cos\theta)\rangle=-1$ relates to the collinear geometry with the Ar atom at the other end of the HCN molecule.

In this regard, we use the notation to label the ArHCN bending states developed previously to describe systems such as ArHCl.[9,14,35] Here, the projection quantum number K, which refers to the projection of the total and rotational angular momentum along the body-fixed z axis **R**, is useful, as are the quantum numbers $\{j\}$ corresponding to the pure rotational states of the monomer molecule. Thus ($j=0$, $K=0$) refers to the ground state level, ($j=1, K=0$) to the "Σ bend" vibration, and ($j=1$, $K=1$) to the "Π bend" vibration of the ArHCN complex. Furthermore, the levels correlating with ($j=2, K=1$ and 0) have been predicted[14] recently to have surprisingly large intensities for excitation from the ground state for ArHCl. This prediction has been verified in near-infrared measurements[36] involving observation of combination bands associated with excitation of the HCl stretch in ArHCl. These "$j=2$" bands will be also of

interest in ArHCN. We emphasize that this notation is used purely for labeling states; j and K are not good quantum numbers in ArHCN. Indeed, as was shown by Bratoz and Martin,[37] the bending modes of an atom–diatom van der Waals complex with a relatively small rotational constant for the monomer molecule might be more accurately described by a harmonic oscillator notation.[35] This aspect is considered further in the discussion section.

III. NUMERICAL PROCEDURES

The small rotational constant of HCN, 1.478 22 cm^{-1}, ensures that it is much harder to obtain converged energy levels for ArHCN than for ArHCl; the magnitudes of the frequencies of the bending modes of the complex are directly related to the size of the monomer rotational constant, and a small bending frequency ensures a stronger interaction between the ground state and bending modes which, in turn, leads to large basis sets being needed to ensure convergence. The current results suggest that it is purely the small rotational constant of the HCN that leads to the observed perturbation in the fundamental energy levels, not any unusual features of the potential energy surface.

The basis set used in the computations reported here had the parameters: $j_{max} = 17, n_t = 89$, $N_{stretch} = 37, N_{bend} = 44$, and $N_X = 46$. The values of $R_a = 6.3$ bohr and $R_b = 24.0$ bohr were used. This gave a final CI matrix to diagonalize of dimension 593 for $J = 0$ and 921 for $J = 1$, with odd parity. The SCF procedure was found to be crucial in obtaining well converged results. Table III gives an example of the energy levels calculated with the CI procedure for 0, 6, 9, and 12 SCF iterations. These tests, and those varying the other parameters, suggest that the mode with lowest energy should have an energy converged to an accuracy within 0.01 cm^{-1}, while the next three levels up should be converged to within 0.05 cm^{-1}. This is a sufficient accuracy to predict the form of the spectrum, but is not accurate enough to give reliable results for centrifugal distortion constants such as D_J.

As the *ab initio* potential surface itself is not expected to be very accurate, the value of the calculations reported here is not in producing spectroscopic constants that compete with those measured in high-resolution spectroscopy, but rather to predict the general appearance of the spectrum, establish which modes can have significant transition intensities, and give descriptions of the character of the rovibrational energies and wave functions in ArHCN. We believe such calculations to be particularly valuable on a system such as ArHCN for which hardly anything is known about the van der Waals bending and stretching modes and no determination has been made of the potential energy surface.

TABLE IV. Calculated energies, $\langle P_1(\cos\theta)\rangle$ and $\langle P_2(\cos\theta)\rangle$ values for rovibrational levels of ArHCN with $J = 0$.

Level	Energy/cm^{-1}	$\langle P_1(\cos\theta)\rangle$	$\langle P_2(\cos\theta)\rangle$
Ground state ($j = 0$)	− 55.9464	0.8228	0.5890
Σ bend ($j = 1, K = 0$)	− 51.7271	− 0.4726	0.1206
$j = 2, K = 0$	− 45.9179	− 0.1246	0.1988
$j = 3, K = 0$	− 40.3736	0.1419	0.2514
Σ stretch ($j = 0$)	− 32.1858	0.4271	0.4491

IV. RESULTS AND DISCUSSION

In Tables IV and V we give the calculated energies and $\langle P_1(\cos\theta)\rangle$ and $\langle P_2(\cos\theta)\rangle$ values for the first few levels of ArHCN with $J = 0$ and 1. We also list the calculated intensities for the $J = 0 \rightarrow 1$ transition in Table V. The results reported in these tables at once illustrate several interesting points.

First, the $J = 0 \rightarrow 1$ frequencies for the transitions from the ground state into the Σ and Π bending vibrations have the very low frequencies of 4.332 and 6.727 cm^{-1}, respectively. The intensities for the transition into the Σ bend are only 0.04 of the intensities for the ground state–ground state transitions. This will make the Σ bend difficult to observe. However, the Π bend has an intensity about 0.12 of the ground state–ground state transition, which should make it observable. These findings correlate quite well with the infrared experimental results of Fraser and Pine.[21] They observe a transition at a frequency displaced by 7.8 cm^{-1} from the C–H stretching frequency in ArHCN that they assign to excitation of the combination band containing the Π bending mode. However they report no observation of a second bending mode. Also, Leopold *et al.* did suggest the frequency

TABLE III. CI calculation of energies of first four rovibrational energy levels of ArHCN as a function of the number of iterations in the SCF procedure.

	SCF iterations			
Mode[a]	0	6	9	12
Ground state ($j = 0$)	− 55.9422[b]	− 55.9456	− 55.9462	− 55.9464
Σ bend ($j = 1, K = 0$)	− 51.6184	− 51.7050	− 51.7198	− 51.7271
Π bend ($J = 1, j = 1, K = 1$)	− 49.0575	[c]	− 49.2085	− 49.2193
$j = 2, K = 0$	− 45.7917	− 45.8920	− 45.9094	− 45.9179

[a] All results are for $J = 0$ in every case except for the Π bend which has $J = 1$ and $p = -1$.
[b] Frequencies are in cm^{-1}.
[c] Not calculated.

TABLE V. Calculated energies, $\langle P_1(\cos\theta)\rangle$ and $\langle P_2(\cos\theta)\rangle$ values for rovibrational energy levels of ArHCN with $J=1$ and $p=-1$. Also shown are the intensities I and the frequencies F for the $J=0\rightarrow 1$ transitions from the ground state.

Level	Energy/cm^{-1}	$\langle P_1(\cos\theta)\rangle$	$\langle P_2(\cos\theta)\rangle$	I	F/cm^{-1}
Ground state ($j=0$)	−55.8494	0.8233	0.5896	0.692	0.0971
Σ bend ($j=1, K=0$)	−51.6144	−0.4736	0.1211	0.036	4.3321
Π bend ($j=1, K=1$)	−49.2193	−0.0212	−0.1372	0.122	6.7271
$j=2, K=0$	−45.8456	−0.0932	0.1991	0.035	10.0918
$j=2, K=1$	−45.1161	0.2267	0.2050	0.090	10.8303
$j=3, K=0$	−40.2833	0.1390	0.2508	0.003	15.6631
$j=3, K=1$	−37.3296	−0.1461	0.1504	0.009	18.6168
Σ stretch ($j=0$)	−32.0963	0.4245	0.4485	0.001	23.8501
Σ stretch ($j=1, K=0$)	−30.6470	0.1725	0.1503	0.007	25.2994

of the bending mode in ArHCN would be close to 10 cm^{-1}.[18]

These variations in transition intensity can be correlated with the $\langle P_1(\cos\theta)\rangle$ values reported in Tables IV and V. This has the value of 0.8235 for the ground state, which corresponds to an angle of $\theta = 35°$. The angles extracted for the Σ and Π bends are 118° and 91°, respectively. Therefore, the Σ bending vibration does not have the Ar atom localized at the same end of the HCN molecule as the ground state, and the transition intensity will be very weak. However, the Π bend corresponds to a perpendicular configuration which is closer to the configuration of the ground state so that the probability of excitation will be quite large. These results are quite similar to those for ArHCl.[14] Here it is found that the θ values deduced from the $\langle P_1(\cos\theta)\rangle$ calculations are 49°, 118°, and 77° for the ground state, Σ bend and Π bend, respectively. Since the ground state is not localized so strongly towards the collinear configuration for ArHCl, the ground state→Σ bend transition is about three times as strong in intensity as that calculated for ArHCN. The reason why the ArHCN ground state is localized more to the collinear configuration is because the bending zero-point energy is smaller than in ArHCl, where the frequencies of the Σ and Π bends are 23.7 and 32.4 cm^{-1}, respectively.[10] This is directly related to the fact that the b rotational constant for HCl is about 7 times that for HCN and simple theories suggest that the bending frequencies should depend linearly on b for very weak anisotropy in the potential and on $b^{1/2}$ for a very strongly anisotropic potential.[35,37]

Examination of the energy levels reported in Table V shows an interesting progression in the bending modes. It can be seen that these are approximately equally spaced by a frequency of about 5 cm^{-1}, with smaller perturbations associated with the K quantum numbers. For a given "j" state, the energy of the $K=0$ levels always fall below the $K=1$ levels. This is because of the double minimum for the bending potential for Ar + HCN with a negative average $c_2(R)$ coefficient. Perturbation theory shows that the $K=0$ levels will have energies below those for $K=1$ under these conditions.[35,37] These results suggest that the energy levels of the ArHCN van der Waals bending modes are closer to the harmonic oscillator limit than to those described by the $bj(j+1)$ formula. This is expected for a system with a large potential anisotropy compared to the b rotational constant.[35] This is in contrast to ArHCl where the large b rotational constant of HCl ensures that the bending energy levels are rather more accurately described by $bj(j+1)$.

These findings also are relevant to the predictions of intensities in ArHCN. It can be seen from Table V that the transitions from the ground state into the ($j=2, K=0$) level has an intensity nearly as large as that for excitation from the ground state into the Π bend. Also, the intensity for excitation into the ($j=2, K=1$) level is nearly the same as that for excitation of the Σ bend. In ArHCl, the $j=0\rightarrow 2$ transition was predicted to be intense enough to be observed[14,36] although the intensities for excitation of the $j=2$ levels are much larger in ArHCN, signifying a major breakdown of the $j=0\rightarrow 1$ "selection rule." It should be noted that, in the harmonic oscillator limit, the intensities for $j=0\rightarrow 2$ transitions will be zero. This suggests that ArHCN is still not very close to that limit.

Observation of the frequency of the intermolecular stretching mode in van der Waals molecules are of particular interest as this information enables bond dissociation energies to be estimated. Our calculations give the intermolecular stretching frequency of ArHCN to be 23.7 cm^{-1}, which is higher than the value of 10 cm^{-1} suggested by Leopold *et al.*[18] Our calculations also suggest that the intensity for excitation of this stretching mode will be very low. However, if the dipole moment of the ArHCN complex was allowed to have a dependence on R then the intensity for excitation of this mode would be much larger. In ArHCl, the intermolecular stretching frequency was 32.4 cm^{-1} and the intensity for excitation of this level was large enough to be observed because of the close proximity in energy of the Π bending mode from which the intermolecular stretch borrowed some intensity.[14] This emphasizes again some important differences between ArHCN and ArHCl.

One of the quantities measured in several of the microwave experiments was $\langle P_2(\cos\theta)\rangle$ for several different J values of the fundamental mode.[18,19] The value of θ inferred from these measurements is found to decrease more significantly in ArHCN than for ArHCl or ArHBr. A comparison of our calculations of $\langle P_2(\cos\theta)\rangle$ with the most recent experimental measurements[19] is shown in Table VI. It can be seen that the calculations are within 5% of the experimental

TABLE VI. Comparison of calculated and measured values of $\langle P_2(\cos\theta)\rangle$ for the ground state of ArHCN.

J	Experimental[a]	Calculation
0	0.6028	0.5890
1	0.6042	0.5896
2	0.6067	0.5909
3	0.6105	0.5924
4	0.6157	0.5931

[a] Reference 19.

values and do show an increase in $\langle P_2(\cos\theta)\rangle$, which implies a decrease in θ. However, the increase in $\langle P_2(\cos\theta)\rangle$ with J is not so strong as that observed in experiment. This suggests that the exact potential energy surface will give even more angular–radial coupling that than obtained in our calculations. The calculated $J=0\rightarrow 1$ transition frequency in the ground state is 0.097 cm^{-1}. This is to be compared with the experimental value[19] of 0.107 cm^{-1}. As expected, the *ab initio* prediction slightly underestimates the observed transition frequency. This is because the *ab initio* calculations normally give a potential that has a well depth that is too small and situated at a larger value of R than the exact case; hence the B rotational constant will be smaller than the exact result. The average value of R deduced from these numbers is $R=4.41$ and 4.64 Å in experiment and calculation, respectively.

The calculated spectrum for excitation of the van der Waals modes of ArHCN over the frequency range up to 25 cm^{-1} is shown in Fig. 2 for a temperature of 1.6 K. All of the transitions in this spectrum are from the ground state energy level. To obtain the microwave and far-infrared spectrum from this figure, the transitions for frequencies less than zero should be ignored. To predict the infrared spectrum for excitation of the CH stretch in ArHCN, it is simply necessary to add 3308.787 cm^{-1} to the calculated frequencies. Figure 2 illustrates many of the features discussed above and presented in the Tables. The ground state–ground state transitions are by far the most intense, followed by the Π bend, with its distinctive Q branch, at 7 cm^{-1}, the highly congested band associated with $j=2$, $K=0$ and $j=2$, $K=1$ close to 10 cm^{-1}, and the Σ bend at 4.5 cm^{-1}. The transitions for excitation of the ($j=3$, $K=0$) and ($j=3$, $K=1$) bands are just discernible at 16 and 18.5 cm^{-1}, respectively. All of the bending modes show considerable distortions in their P and R branches.

This feature is illustrated in more detail in Figs. 3–5 in which the calculated spectra for excitation of the Σ bend, Π bend, and $j=2$ levels are shown, respectively, at high resolution. The spectrum for the Π bend in particular shows considerable distortion, which is made more complicated by the Q branch running into the R branch. This is due to the strong

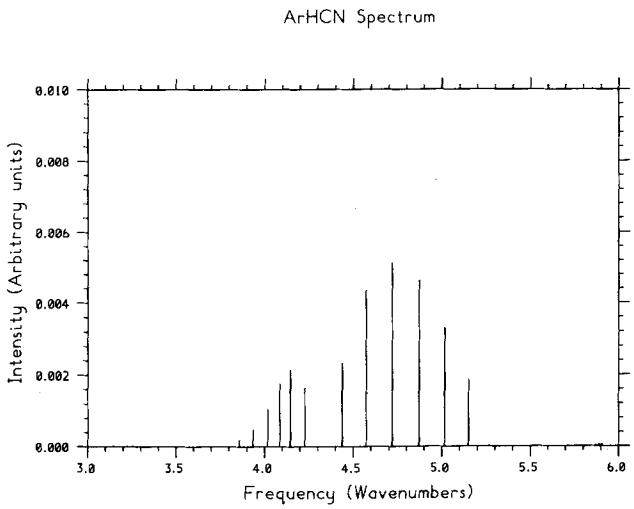

FIG. 3. Calculated high-resolution spectrum for excitation of the Σ-bend vibration in ArHCN around 4.5 cm^{-1} at 1.6 K.

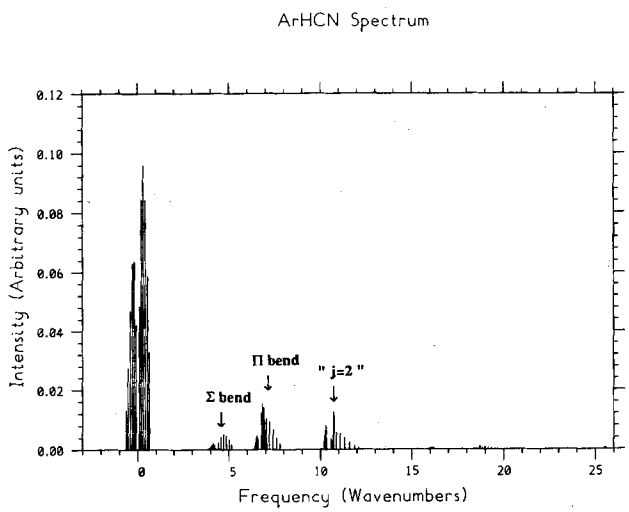

FIG. 2. Calculated spectrum for exciting the van der Waals modes of ArHCN over the frequency range up to 25 cm^{-1} with an ArHCN internal temperature of 1.6 K.

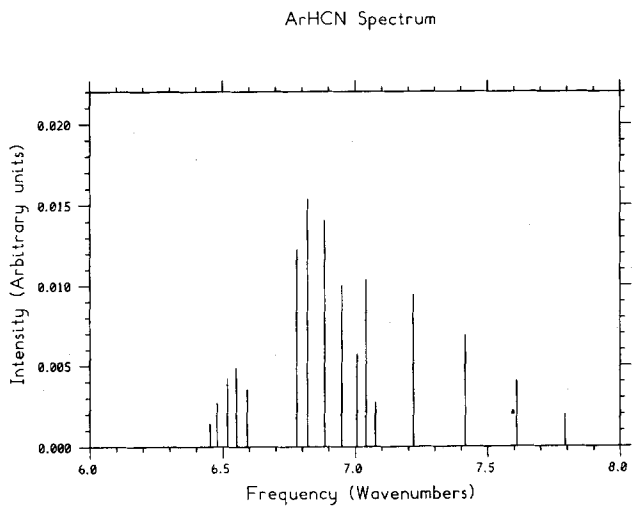

FIG. 4. Calculated high-resolution spectrum for excitation of the Π-bend vibration in ArHCN around 7.0 cm^{-1} at 1.6 K.

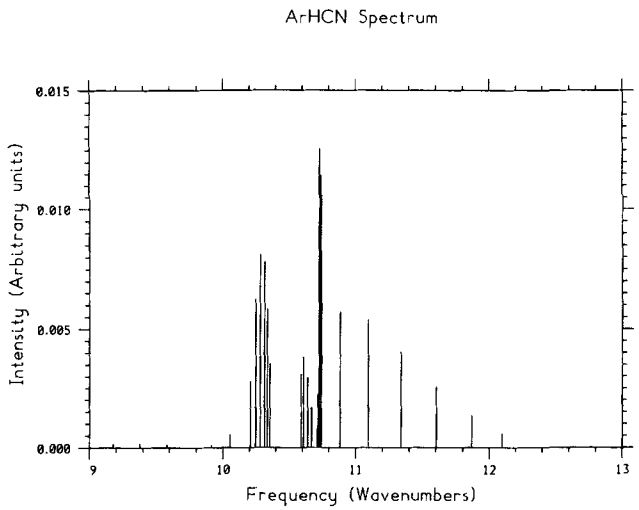

FIG. 5. Calculated high-resolution spectrum for excitation of the $j = 2$, doubly excited bending vibrations in ArHCN around 11 cm^{-1} at 1.6 K.

interaction between the Π and Σ bends that pushes up the energies of the Π^+ bending levels, while having no effect on the Π^- levels [here, Π^+ and Π^- refer to the spectroscopic parity $(-1)^J p$]. Also, the P branch of the Π bend has much lower intensities than the R branch, which is illustrative of strong perturbations between two modes which produces interference effects in the line intensities. Similar effects are seen in ArHCl, but the perturbative effects are not so strong there.[12] The $j = 2$ spectra of Fig. 5 are most strongly perturbed as here the $(j = 2, K = 0)$ and $(j = 2, K = 1)$ levels are coupled by Coriolis coupling and are also coupled to the Σ and Π bends and the $j = 3$ levels. The P branch of the $(j = 2, K = 0)$ level has very small intensities, whereas the R branch intensities around 10.3 cm^{-1} are relatively strong. The P branch of the $(j = 2, K = 1)$ band also has a bandhead. The intense Q branch of the $(j = 2, k = 1)$ band is centered at 10.7 cm^{-1}. The $j = 2$ levels in ArHCl also show somewhat similar distortions and irregularities in line intensities.[14,36]

The most unexpected prediction from these calculated spectra on ArHCN is the surprisingly large intensity of the "$j = 2$" lines above 10 cm^{-1}. This suggests that if the infrared experiment on ArHCN could be repeated for frequencies over 10 cm^{-1} above the C–H stretching frequency then new lines might be seen. It should be mentioned here that the equivalent $j = 2$ lines in ArHCl were first predicted to have intensities large enough to be measured[14] and this lead to the subsequent first measurement of the spectra for excitation of these levels in which combination bands associated with excitation of the doubly excited bending mode and the HCl stretch in ArHCl were observed.[36]

In comparing the calculated spectra with those observed by Fraser and Pine at a frequency displaced by about 8 cm^{-1} from the CH stretching frequency in ArHCN,[21] it is important to note that our calculated intensity of the lines in the Q branch for excitation of the Π bend are larger than those for the R branch. In the experiment,[21] if it is the combination band containing the Π bend that is observed, then the Q branch has an intensity much smaller than the R branch. This does not seem to be in agreement with our findings. However, no P branch was observed in the infrared measurements, and we do predict the P branch to have intensities much smaller than the R branch. Overall, our results do provide some evidence to suggest that Fraser and Pine were observing a transition involving excitation into the combination band involving simultaneous excitation of the CH stretch and Π bending mode in ArHCN, but more experimental results are needed. It might also be possible to observe the spectrum for analogous combination bands involving excitation of the HCN vibrational bending mode in ArHCN which has quite a strong intensity.[38]

V. CONCLUSIONS

An *ab initio* calculation has been performed of the spectrum for excitation of the van der Waals modes in the weakly bound complex ArHCN. The potential energy surface has been calculated using the CEPA-1 method, and the rovibrational bound states are calculated using a variational basis set SCF-CI procedure.

The potential energy surface calculated is rather similar to that for ArHCl, having a double minimum potential with respect to the bending angle. However, the relatively small rotational constant of the HCN monomer ensures that the van der Waals spectrum for ArHCN has some differences compared to that for ArHCl. In particular, the bending modes have quite small frequencies which perturb the ground state, and also produce some irregular features in the line positions and intensities for excitation of the van der Waals modes. Furthermore, the calculations suggest that it should be possible to observe modes with at least two quanta of excitation in the van der Waals bending mode. The energies of the ArHCN bending modes are closer to harmonic oscillators than those for ArHCl. The calculated spectra for ArHCN have been compared with infrared experimental data[21] and do provide extra evidence to suggest that the experimentally observed combination band displaced 7.8 cm^{-1} from the C–H fundamental stretching transition correlates with excitation of the Π bending mode in ArHCN. However, more experimental infrared and far-infrared spectra on ArHCN will be worthwhile.

ArHCN is the fourth system for which we have calculated the van der Waals spectrum using the *ab initio* (CEPA-1) method for the potential energy surface and a variational basis set method for the rovibrational bound states, with bond lengths of the monomer molecules held fixed. The previous systems we have studied with this approach are NeHF, H_2HF, and ArOH. Calculations such as these are not expected to give results that compete in accuracy with those obtained in high-resolution spectroscopy. Their contribution is in simulating the spectra for excitation of the van der Waals modes, determining the nature of the rovibrational bound states and predicting the intensities for excitation of different modes. The calculations do often suggest new experimental investigations that might be worthwhile. Although the calculated potential energy surfaces are not definitive they are a good starting point for further refinements and are often the best that is available in the absence of good experimental data. Above all, the *ab initio* approach enables

predictions to be made on new systems, such as ArHCN, for which no experimental data exists in certain regions of the spectrum.

ACKNOWLEDGMENTS

Help from Dr. P. J. Knowles with the CEPA calculations is gratefully acknowledged. The *ab initio* calculations were done with the MOLPRO Program developed by Lim and H.-J. Werner. This work also benefited from useful discussions with W. Klemperer and G. T. Fraser. This work was supported by the Science and Engineering Research Council and NATO.

[1] *Structure and Dynamics of Weakly Bound Complexes*, edited by A. Weber (Reidel, Dordrecht, 1987); *Dynamics of Polyatomic Van der Waals Complexes*, edited by N. Halberstadt and K. C. Janda (Plenum, New York, 1990).
[2] D. J. Nesbitt, Chem. Rev. **88**, 843 (1988).
[3] R. J. Le Roy and J. S. Carley, Adv. Chem. Phys. **42**, 353 (1980).
[4] J. M. Hutson, J. Chem. Phys. **89**, 4550 (1988).
[5] J. M. Hutson, J. Chem. Phys. **91**, 4448 (1989).
[6] J. M. Hutson, J. Chem. Phys. **91**, 4455 (1989).
[7] D. J. Nesbitt, M. S. Child, and D. C. Clary, J. Chem. Phys. **90**, 4855 (1989).
[8] S. E. Novick, P. Davies, S. J. Harris, and W. Klemperer,J. Chem. Phys. **59**, 2273 (1973).
[9] M. D. Marshall, A. Charo, H. O. Leung, and W. Klemperer, J. Chem. Phys. **83**, 4924 (1985).
[10] D. Ray, R. L. Robinson, D.-H. Gwo, and R. J. Saykally, J. Chem. Phys. **84**, 1171 (1986); R. L. Robinson, D. Ray, D.-H. Gwo, and R. J. Saykally, *ibid.* **87**, 5156 (1987); R. L. Robinson, D.-H. Gwo, D. Ray, and R. J. Saykally, *ibid.* **86**, 5211 (1987); R. L. Robinson, D.-H. Gwo, and R. J. Saykally, *ibid.* **87**, 5156 (1987).
[11] C. M. Lovejoy and D. J. Nesbitt, J. Chem. Phys. **91**, 2790 (1989).
[12] C. M. Lovejoy and D. J. Nesbitt, Chem. Phys. Lett. **146**, 582 (1988).
[13] C. M. Lovejoy and D. J. Nesbitt, Chem. Phys. Lett. **147**, 490 (1988).
[14] D. C. Clary and D. J. Nesbitt, J. Chem. Phys. **90**, 7000 (1989).
[15] D. C. Clary, C. M. Lovejoy, S. V. ONeil, and D. J. Nesbitt, Phys. Rev. Lett. **61**, 1576 (1988); S. V. ONeil, D. J. Nesbitt, R. Rosmus, H.-J. Werner, and D. C. Clary, J. Chem. Phys. **91**, 711 (1989); D. J. Nesbitt, C. M. Lovejoy, T. G. Lindeman, S. V. ONeil, and D. C. Clary, *ibid.* **91**, 722 (1989).
[16] A. S. Pine, W. J. Lafferty, and B. J. Howard, J. Chem. Phys. **81**, 2929 (1984); B. J. Howard and A. S. Pine, Chem. Phys. Lett. **122**, 1 (1985).
[17] E. J. Campbell, L. W. Buxton, and A. C. Legon, J. Chem. Phys. **78**, 3483 (1983).
[18] K. R. Leopold, G. T. Fraser, F. J. Lin, D. D. Nelson, Jr., and W. Klemperer, J. Chem. Phys. **81**, 4922 (1984).
[19] T. D. Klots, C. E. Dykstra, and H. S. Gutowsky, J. Chem. Phys. **90**, 30 (1989).
[20] R. E. Bumgarner and G. A. Blake, Chem. Phys. Lett. **161**, 308 (1989).
[21] G. T. Fraser and A. S. Pine, J. Chem. Phys. **91**, 3319 (1989).
[22] D. C. Clary and P. J. Knowles, J. Chem. Phys. **93**, 6334 (1990).
[23] C. Chakravarty, D. C. Clary, A. Degli Esposti, and H.-J. Werner, J. Chem. Phys. **93**, 3367 (1990).
[24] D. C. Clary, C. Chakravarty, and A. R. Tiller, in *Dynamics of Polyatomic Van der Waals Complexes*, edited by N. Halberstadt and K. C. Janda (Plenum, New York, 1990), p. 355.
[25] W. Meyer, J. Chem. Phys. **58**, 1017 (1973).
[26] J. M. Bowman, Acc. Chem. Res. **19**, 202 (1986).
[27] M. A. Ratner and R. B. Gerber, J. Phys. Chem. **90**, 20 (1986).
[28] P. R. Bunker, T. Carrington Jr., P. C. Gomez, M. D. Marshall, M. Kofranek, H. Lischka, and A. Karpfen, J. Chem. Phys. **91**, 5154 (1989).
[29] C. G. Gray and K. E. Gubbins, *The Theory of Molecular Fluids* (Clarendon, Oxford, 1984).
[30] A. M. Arthurs and A. Dalgarno, Proc. R. Soc. London Ser. A **256**, 540 (1960).
[31] S. F. Boys and F. Bernadi, Mol. Phys. **19**, 553 (1970).
[32] A. D. Buckingham, P. W. Fowler, and J. M. Hutson, Chem. Rev. **88**, 963 (1988).
[33] I. P. Hamilton and J. C. Light, J. Chem. Phys. **84**, 306 (1986).
[34] D. M. Brink and G. R. Satchler, *Angular Momentum* (Clarendon, Oxford, 1968).
[35] J. M. Hutson, in *Advances in Molecular Vibrations and Collision Dynamics* (to be published).
[36] D. J. Nesbitt, Faraday Discuss. Chem. Soc. **86**, 33 (1988).
[37] S. Bratoz and M. L. Martin, J. Chem. Phys. **42**, 1051 (1965).
[38] G. Herzberg, *Infrared and Raman Spectra* (Van Nostrand, New York, 1945).